

Morphological statistics and their applications in cosmology



Pravabati Chingangbam

IIA, Bengaluru

©IIT Madras

Pic: SDSS

CMB: $\lambda \sim 1$ mm

$$\delta T(\theta, \phi), \quad \Phi(\theta, \phi)$$

Hydrogen: $\lambda \geq 21$ cm

$$\delta T_B(\theta, \phi, z)$$

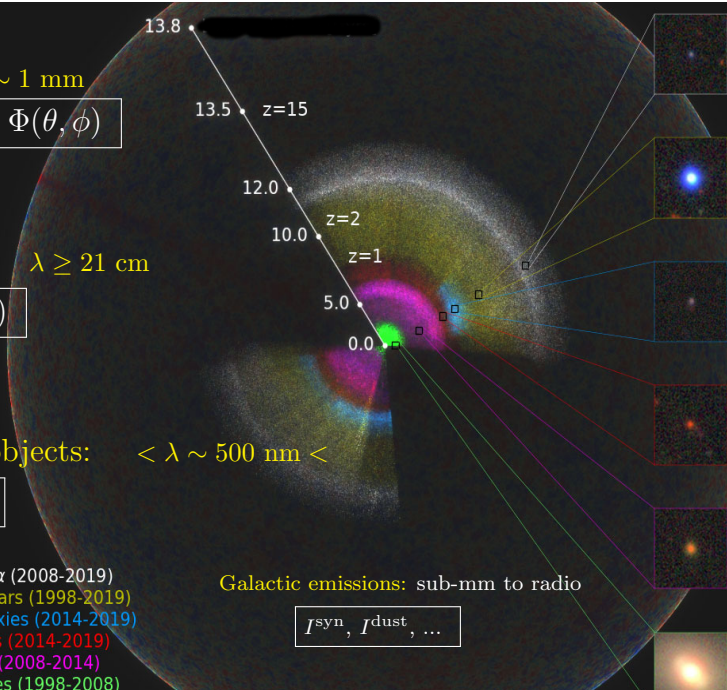
Collapsed objects: $< \lambda \sim 500$ nm $<$

$$\delta \rho(\theta, \phi, z)$$

eBOSS + BOSS Lyman- α (2008-2019)
eBOSS + SDSS I-II Quasars (1998-2019)
eBOSS Young Blue Galaxies (2014-2019)
eBOSS Old Red Galaxies (2014-2019)
BOSS Old Red Galaxies (2008-2014)
SDSS I-II Nearby Galaxies (1998-2008)

Galactic emissions: sub-mm to radio

$$I^{\text{syn}}, I^{\text{dust}}, \dots$$



Cosmological observables as random fields

Neyman & Scott 1957: *“.. considerable progress and aesthetic gain may be expected if determinism is abandoned and replaced by a frank probabilistic treatment of cosmology. This requires the adoption of the view that the Universe is a realization of a stochastic process which is stationary in the three (spatial) co-ordinates (cosmological principal) and possibly also stationary in the fourth (time) co-ordinate (“perfect” cosmological principle).”*

Quantum fluctuations during inflation (Mukhanov & Chibisov 1981): \Rightarrow primordial density fluctuations.

Physical interactions - evolve the primordial fields to what we observe.

Much of modern cosmology has been the study of the statistics of density fluctuations.

Overview of random fields

Field: $f(\mathbf{x}, t)$

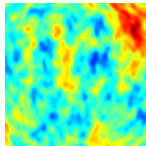
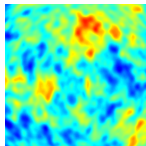
Probability distribution: $\mathcal{P} \left[f(\mathbf{x}_1), f(\mathbf{x}_2), \dots, f(\mathbf{x}_k) \right]$

n -point correlation functions:

2-point fn $\rightarrow \xi(\mathbf{x}_1, \mathbf{x}_2) \equiv \left\langle f(\mathbf{x}_1) f(\mathbf{x}_2) \right\rangle$

3-point fn $\rightarrow \left\langle f(\mathbf{x}_1) f(\mathbf{x}_2) f(\mathbf{x}_3) \right\rangle$

.....



Gaussian field:

$$\mathcal{P} \left[f(\mathbf{x}_1), f(\mathbf{x}_2), \dots, f(\mathbf{x}_k) \right] = \frac{1}{\sqrt{(2\pi)^k \mathbf{Det} \xi}} \exp \left(-\frac{1}{2} F^T \xi^{-1} F \right),$$

$$F \equiv (f(\mathbf{x}_1), f(\mathbf{x}_2), \dots, f(\mathbf{x}_k))$$

Random fields in cosmology

Cosmological principle - Homogeneity and isotropy

- All positions and directions are equivalent.
- All n -point correlation functions depend only on the spatial separations.

Assume ergodicity

The Universe corresponds to **one realization** of a random field.

Ensemble expectation \iff Volume average.

Random fields in cosmology - data and theory

Testing Theory:

- ① Fundamental assumptions
- ② Theoretical framework - the equations - Einstein's equations, Boltzman equations for different matter components
- ③ Theoretical Parameters -
- ④ Nature of primordial fluctuations - gravity and quantum field equations, nature of interactions
- ⑤

Need to construct **good Statistics** to compare data and theory.

2-point function as a cosmological tool

Correlation function \iff Power spectrum

Example - CMB angular power spectrum

$$T(\hat{n}) = T_0 + \Delta T(\hat{n}), \quad \Delta T(\hat{n}) = \sum_{\ell m} a_{\ell m} Y_{\ell m}(\hat{n})$$

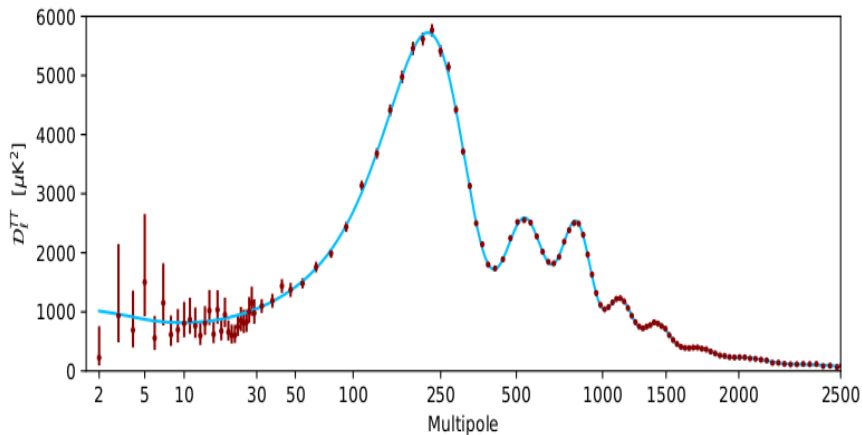
Then

$$C_{\ell}^{\text{obs}} = \frac{1}{\ell(\ell+1)} \sum |a_{\ell m}|^2$$

$$C_{\ell}^{\text{theory}} \sim \int dk k^2 |\Delta_{\ell}(k, t_0)|^2 P(k) \longrightarrow C_{\ell}^{\text{theory}} \left(\Omega_i, H_0, \tau, \dots \right)$$

2-point function as a cosmological tool

$$D_\ell^{\text{obs}} \equiv \ell(\ell + 1)C_\ell$$



Beyond 2-point function

Much more information in observed data than revealed by 2-point function. Timely to expand our toolset.

Options:

① Higher order n -point functions

- ▶ Non-Gaussian fields: higher n -point functions contain independent information.

But: expensive to compute and analyze.

Require: efficient algorithms that can improve the computation time

E.g. Philcox & Slepian, arxiv:2106.10278

② **Alternative:** geometry and topology of random fields

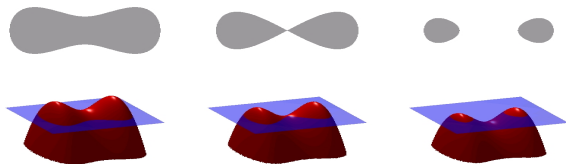
Geometry and topology of random fields

Morse theory - from differentiable functions to topology

- Connectivity, Extrema counts - maximas, minimas, saddles

Integral geometry - Minkowski tensors

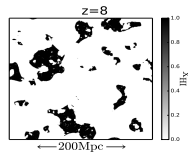
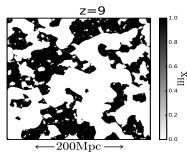
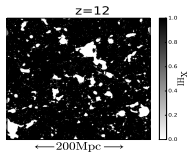
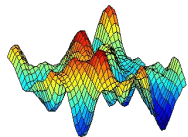
- Area, perimeter, counts, Euler characteristic, Betti numbers, anisotropy, alignment, total curvature



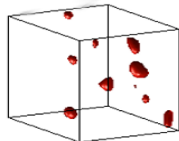
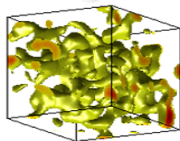
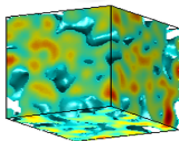
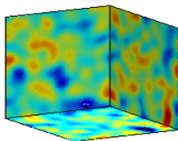
Pic: Oleg Alexandrov

Excursion sets of random fields

2 dimensions:



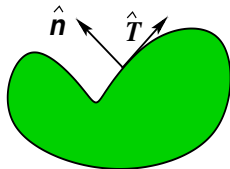
3 dimensions:



3D picture: R. Adler

Rich geometrical and topological structure

Minkowski tensors in 2D



$$W_0^m = \int_A \vec{r}^m da,$$

$$W_1^{m,n} = \int_C \vec{r}^m \otimes \hat{n}^n ds,$$

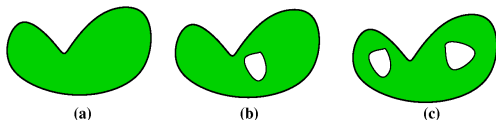
$$W_2^{m,n} = \int_C \vec{r}^m \otimes \hat{n}^n \kappa ds$$

$\kappa = \text{Curvature}$

Minkowski tensors in 2D

Dim	Rank 0	Rank 1	Rank 2	
			Translation covariant	Translation invariant
4	–	–	$W_0^{2,0}$	–
3	–	$W_0^{1,0}$	$W_1^{2,0}$	–
2	W_0	$W_1^{1,0}$	$W_2^{2,0}$	$W_1^{1,1}$
1	W_1	$W_2^{1,0}$ $W_1^{0,1}$,		$W_1^{0,2}$, $W_2^{1,1}$
0	W_2	$W_2^{0,1}$,	–	$W_2^{0,2}$

Physical meaning



RANK 0

$W_0 = \int da$	Area
$W_1 = \int ds$	Perimeter
$W_2 = \int \kappa ds$	Counts - Betti numbers, Euler characteristic

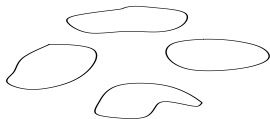
$$b_c \equiv \frac{1}{2\pi} \int_{C_+} \kappa ds, \quad b_v \equiv \frac{1}{2\pi} \int_{C_-} \kappa ds, \quad g = b_c - b_v.$$

RANK 2, translation invariant

$W_1^{1,1} = \int_C \vec{r} \otimes \hat{n} ds$	$= W_0 \times I$
$W_1^{0,2} = \int_C \hat{n} \otimes \hat{n} ds$	Trace gives W_1 , 3 degrees of freedom.
$W_2^{0,2} = \int_C \hat{n} \otimes \hat{n} \kappa ds$	$= W_2 \times I$

Shape and alignment information

Eigenvalues of $W_1^{0,2}$ give information of anisotropy and alignment.



Calculate $W_1^{0,2}$ for each curve. Calculate eigenvalues λ_1, λ_2 and take ratio.

$$\beta \equiv \frac{\lambda_1}{\lambda_2}$$

Sum $W_1^{0,2}$ for all curves. Calculate eigenvalues Λ_1, Λ_2 and take ratio.

$$\alpha \equiv \frac{\Lambda_1}{\Lambda_2}$$

Minkowski tensors for random fields

$$\vec{n} = \nabla f, \quad \kappa = \frac{2f_{;1}f_{;2}f_{;12} - uf_{;1}^2f_{;22} - f_{;2}^2f_{;11}}{|\nabla f|^3}.$$

$$W_1^{0,2} = \frac{1}{4} \int \hat{n} \otimes \hat{n} \, ds = \frac{1}{4} \int_S da \, \delta(u - \nu) \frac{1}{|\nabla u|} \mathcal{M},$$

$$W_2^{0,2} = \frac{1}{2\pi} \int \hat{n} \otimes \hat{n} \, \kappa \, ds = \frac{1}{2\pi} \int_S da \, \delta(f - \nu) \frac{\kappa}{|\nabla f|} \mathcal{M},$$

$$\mathcal{M} = \begin{pmatrix} f_{;1}^2 & f_{;1}f_{;2} \\ f_{;1}f_{;2} & f_{;2}^2 \end{pmatrix}.$$

Minkowski tensors for Gaussian isotropic fields

PC, Yogendran et al 2017

If f is Gaussian then $f_{;i}$ are also Gaussian fields.

The joint PDF of $\mathbf{X} \equiv (f, f_{;1}, f_{;2}, f_{;11}, f_{;12}, f_{;22})$ is given by the Gaussian form

$$P(\mathbf{X}) = \frac{1}{\sqrt{2\pi \text{Det}\Sigma}} \exp\left(-\frac{1}{2}\mathbf{X}^T \Sigma^{-1} \mathbf{X}\right),$$

where Σ is the covariance matrix

$$\Sigma = \langle X_i X_j \rangle$$

For any statistic, $B(\mathbf{X})$, the ensemble expectation is then

$$\langle B(\mathbf{X}) \rangle = \int D[\mathbf{X}] P(\mathbf{X}) B$$

Minkowski tensors for Gaussian isotropic fields

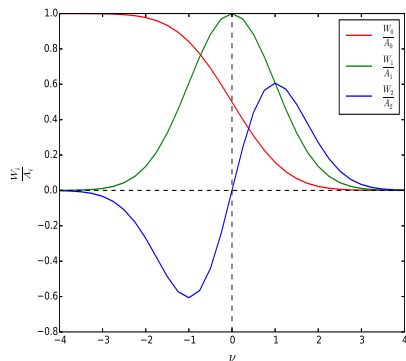
PC, Yogendran et al 2017

$$W_0 = \frac{1}{2} \operatorname{Erfc}(\nu/\sqrt{2})$$

$$\langle W_1^{0,2}(\nu) \rangle \propto \frac{1}{r_c} e^{-\nu^2/2} \times I \times \text{Area}$$

$$\langle W_2^{0,2}(\nu) \rangle \propto \frac{1}{r_c^2} \nu e^{-\nu^2/2} \times I \times \text{Area}$$

$$r_c = \frac{\sigma_0}{\sigma_1}$$



Analytic expressions for Betti numbers and shape parameter β are NOT known as yet.

Information content of Minkowski tensors

r_c contains cosmological information of kinematic properties of universe.

Functional dependence on ν gives information of the nature of the field.

Provides valuable shape and alignment information - clustering and filamentary nature of fields.

Encodes information of time evolution of fields.

Caveats

Good signal to noise of observed data is crucial.

Data must have good resolution in order to resolve structures.

Testing the Cosmological principle

- Look for direction dependence of the power spectrum.
E.g. BiPosh \rightarrow Applied to CMB data.

Souradeep+

- Measure dipole
E.g. Applied to quasar number counts.

Ellis & Baldwin 1984, Singhal 2011, Secret et al 2021,...

- Galaxy cluster scaling relations

Migkas & Reiprich 2018, 2020 . . .

-
- **Propose a new test based on**

*If the field is homogeneous and isotropic we can construct a **geometric object** which is invariant under translations and rotations.*

Measure of anisotropy - finite sampling effect

$$W_2^{0,2} = \begin{pmatrix} \tau + g_1 & g_2 \\ g_2 & \tau - g_1 \end{pmatrix}$$

$$\tau = \text{Trace}$$

$$g = \sqrt{g_1^2 + g_2^2}$$

$$\varphi = \frac{1}{2} \tan^{-1} \frac{g_2}{g_1}$$

$$\alpha \equiv \frac{\Lambda_1}{\Lambda_2} \simeq 1 - \frac{g}{2\tau}$$

φ \Rightarrow orientation of the anisotropy.

g, α \Rightarrow coordinate independent measure of intrinsic anisotropy.

Finite sampling - breaks isotropy

PC, Goyal, Yogendran & Appleby (2021)

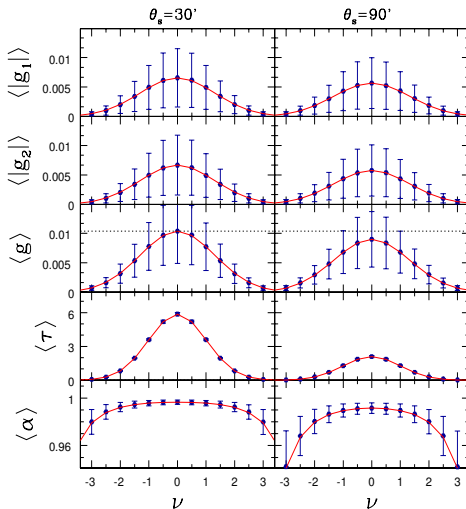
$$\langle |g_1(\nu)| \rangle = A_{g_1} e^{-\nu^2/2\sigma_{g_1}^2}$$

$$\langle |g_2(\nu)| \rangle = A_{g_2} e^{-\nu^2/2\sigma_{g_2}^2}$$

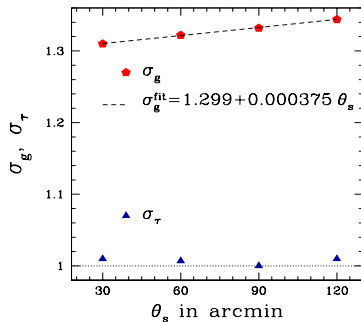
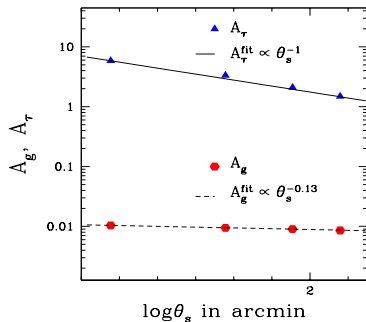
$$\langle g(\nu) \rangle = A_g e^{-\nu^2/2\sigma_g^2}$$

$$\langle \tau(\nu) \rangle = A_\tau e^{-\nu^2/2\sigma_\tau^2}$$

$$\langle \alpha(\nu) \rangle \simeq 1 - \frac{A_g}{A_\tau} e^{\nu^2/2\Delta_g}$$



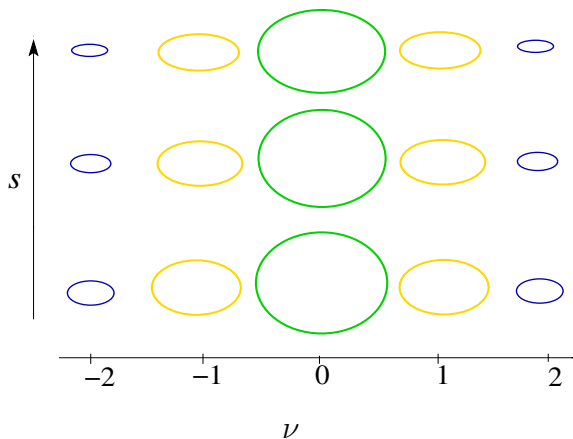
Finite sampling - breaks isotropy



⇒ The amplitudes of τ and g exhibit power law scaling with smoothing.

⇒ σ_g increases linearly with smoothing scale.

Representation of a random field as series of ellipses



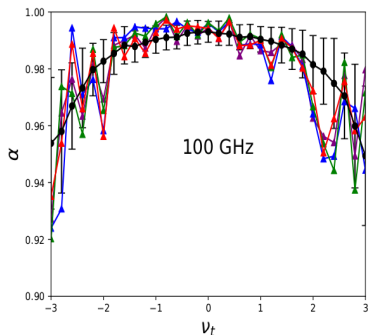
s = resolution parameter

Applications to PLANCK data

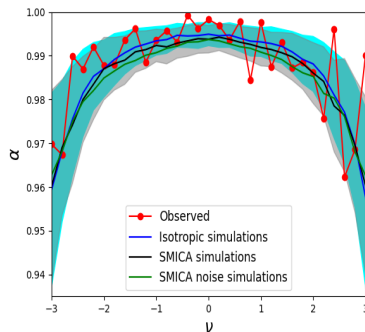
1. PLANCK temperature and E-mode data

Joby Kochappan *et al.*, 2018; 2020

Temperature

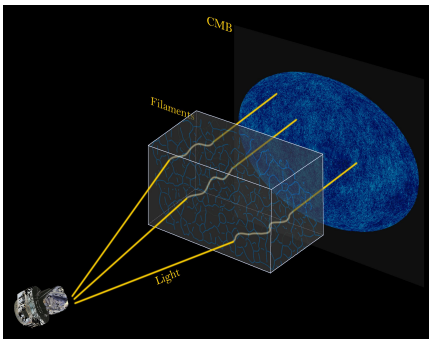


E-mode



Conclusion : No statistically significant deviation from SI.

2. PLANCK convergence map



Pic: He, Alam, Chen & Planck/ESA

$$T^L(\hat{n}') = T^{UL}(\hat{n} + \vec{d})$$

$$\vec{d}(\theta, \phi) = \nabla_{\hat{n}} \Phi$$

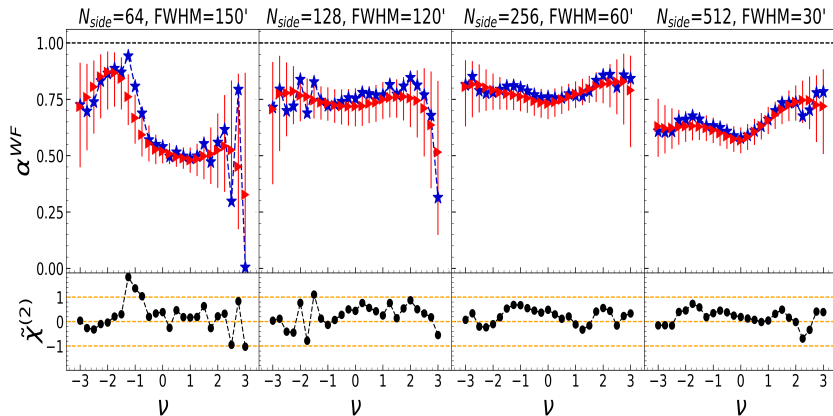
Φ is the Lensing potential.

$$\Phi(\hat{n}) = -2 \int_0^{\chi^*} d\chi \left(\frac{\chi^* - \chi}{\chi \chi^*} \right) \psi(\chi \hat{n}; \eta_0 - \chi)$$

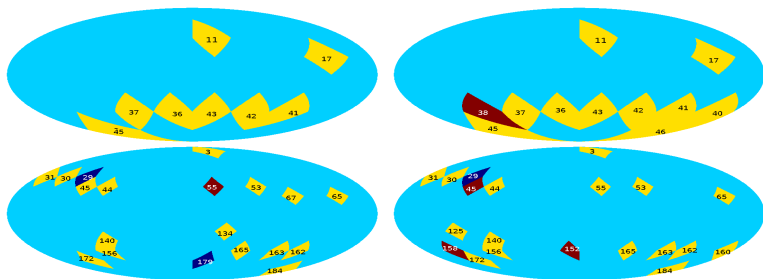
$$\kappa = \nabla^2 \Phi = \text{Convergence}$$

Planck convergence map - global analysis

Priya Goyal & PC 2021



Planck convergence map - patch analysis



Conclusion

- Most anomalous patches have α **higher** than expected.
⇒ Inaccurate instrument noise.
- 2 patches have α **lower** than expected.
⇒ True departure from isotropy.
Further probe needed to isolate the cause.

Summary

- Increasing availability of observational data make it timely to develop tools beyond power spectra for extracting cosmological information.
- Geometry and topology of random fields open up diverse new avenues for data analysis. Analytic predictions to a large extent.

Examples → Minkowski tensors and Betti numbers.

- Constructed a test for statistical isotropy of the Planck data. Identified sky regions that exhibit anomalous behaviour.